# Tracking Points on Deformable Objects Using Curvature Information*

*Isaac COHEN, Nicholas AYACHE, Patrick SULGER*

INRIA, Rocquencourt
B.P. 105, 78153 Le Chesnay CEDEX, France.
Email isaac@bora.inria.fr, na@bora.inria.fr.

## Abstract

The objective of this paper is to present a significant improvement to the approach of Duncan et al. [1, 8] to analyze the deformations of curves in sequences of 2D images. This approach is based on the paradigm that high curvature points usually possess an anatomical meaning, and are therefore good landmarks to guide the matching process, especially in the absence of a reliable physical or deformable geometric model of the observed structures.

As Duncan's team, we therefore propose a method based on the minimization of an energy which tends to preserve the matching of high curvature points, while ensuring a smooth field of displacement vectors everywhere.

The innovation of our work stems from the explicit description of the mapping between the curves to be matched, which ensures that the resulting displacement vectors actually map points belonging to the two curves, which was not the case in Duncan's approach.

We have actually implemented the method in 2-D and we present the results of the tracking of a heart structure in a sequence of ultrasound images.

## 1 Introduction

Non-rigid motion of deformable shapes is becoming an increasingly important topic in computer vision, especially for medical image analysis. Within this topic, we concentrate on the problem of tracking deformable objects through a time sequence of images.

The objective of our work is to improve the approach of Duncan et al. [1, 8] to analyze the deformations of curves in sequences of 2D images. This approach is based on the paradigm that high curvature points usually possess an anatomical meaning, and are therefore good landmarks to guide the matching process. This is the case for instance when deforming patients skulls (see for instance [7, 9]), or when matching patient faces taken at different ages, when matching multipatients faces, or when analyzing images of a beating heart. In these cases, many lines of extremal curvatures (or ridges) are stable features which can be reliably tracked between the images (on a face they will correspond to the nose, chin and eyebrows ridges for instance, on a skull to the orbital, sphenoid, falx, and temporal ridges, on a heart ventricle to the papillary muscle etc...).

As Duncan's team, we therefore propose a method based on the minimization of an energy which tends to preserve the matching of high curvature points, while ensuring a smooth field of displacement vectors everywhere.

The innovation of our work stems from the explicit description of the mapping between the curves to be matched, which ensures that the resulting displacement vectors actually

* This work was partially supported by Digital Equipment Corporation.

map points belonging to the two curves, which was not the case in Duncan's approach. Moreover, the energy minimization is obtained through the mathematical framework of Finite Element analysis, which provides a rigorous and efficient numerical solution. This formulation can be easily generalized in 3-D to analyze the deformations of surfaces.

Our approach is particularly attractive in the absence of a reliable physical or deformable geometric model of the observed structures, which is often the case when studying medical images. When such a model is available, other approaches would involve a parametrization of the observed shapes [14], a modal analysis of the displacement field [12], or a parametrization of a subset of deformations [3, 15]. In fact we believe that our approach can always be used when some sparse geometric features provide reliable landmarks, either as a preprocessing to provide an initial solution to the other approaches, or as a post-processing to provide a final smoothing which preserves the matching of reliable landmarks.

## 2 Modelling the Problem

Let $C_P$ and $C_Q$ be two boundaries of the image sequence, the contour $C_Q$ is obtained by a non rigid (or elastic) transformation of the contour $C_P$. The curves $C_P$ and $C_Q$ are parameterized by $P(s)$ and $Q(s')$ respectively.

The problem is to determine for each point $P$ on $C_P$ a corresponding point $Q$ on $C_Q$. For doing this, we must define a similarity measure which will compare locally the neighborhoods of $P$ and $Q$.

As explained in the introduction, we assume that points of high curvature correspond to stable salient regions, and are therefore good landmarks to guide the matching of the curves. Moreover, we can assume as a first order approximation, that the curvature itself remains invariant in these regions. Therefore, we can introduce an energy measure in these regions of the form:

$$E_{curve} = \frac{1}{2} \int_{\delta S} \left(K_Q(s') - K_P(s)\right)^2 ds \tag{1}$$

where $K_P$ and $K_Q$ denote the curvatures and $s$, $s'$ parameterize the curves $C_P$ and $C_Q$ respectively. In fact, as shown by [8, 13], this is proportional to the energy of deformation of an isotropic elastic planar curve.

We also wish the displacement field to vary smoothly around the curve, in particular to insure a correspondence for points lying between two salient regions. Consequently we consider the following functional (similar to the one used by Hildreth to smooth a vector flow field along a contour [11]) :

$$E = E_{curve} + R\, E_{regular} \tag{2}$$

where

$$E_{regular} = \int_{C_P} \left\| \frac{\partial (Q(s') - P(s))}{\partial s} \right\|^2 ds$$

measures the variation of the displacement vector $\mathbf{PQ}$ along the curve $C_P$, and the $\|.\|$ denotes the norm associated to the euclidean scalar product $\langle ., . \rangle$ in the space $\mathbb{R}^2$.

The regularization parameter $R(s)$ depends on the shape of the curve $C_P$. Typically, $R$ is inversely proportional to the curvature at $P$, to give a larger weight to $E_{curve}$ in salient regions and conversely to $E_{regular}$ to points inbetween. This is done continuously without annihiling totally the weight of any of these two energies (see [4]) .

## 3 Mathematical Formulation of the Problem

Given two curves $C_P$ and $C_Q$ parameterized by $s \in [0,1]$ and $s' \in [0,\alpha]$ (where $\alpha$ is the length of the curve $C_Q$), we have to determine a function $f : [0,1] \rightarrow [0,\alpha]; \quad s \rightarrow s'$ satisfying

$$f(0) = 0 \text{ and } f(1) = \alpha \tag{3}$$

and

$$f = ArgMin(E(f)) \tag{4}$$

where

$$E(f) = \int_{C_P} (K_Q(f(s)) - K_P(s))^2 \, ds + R \int_{C_P} \left\| \frac{\partial (Q(f(s)) - P(s))}{\partial s} \right\|^2 ds \tag{5}$$

The condition (3) means that the displacement vector is known for one point of the curve. In the model above defined we assumed that:

- the boundaries have already been extracted,
- the curvatures $K$ are known on the pair of contours (see [9]).

These necessary data are obtained by preprocessing the image sequence (see for more details [4]).

The characterization of a function $f$ satisfying $f = ArgMin(E(f))$ and the condition (3) is performed by a variational method. This method characterizes a local minimum $f$ of the functional $E(f)$ as the solution of the Euler-Lagrange equation $\nabla E(f) = 0$, leading to the solution of the partial differential equation:

$$\begin{cases} f'' \, \|Q'(f)\|^2 + K_P \langle N_P, Q'(f) \rangle + \frac{1}{R} [K_P - K_Q(f)] \, K'_Q(f) = 0 \\ + \text{ Boundary conditions (i.e. condition 3).} \end{cases} \tag{6}$$

where $Q$ is a parametrization of the curve $C_Q$, $Q'(f)$ the tangent vector of $C_Q$, $K'_Q$ the derivative of the curvature of the curve $C_Q$ and $N_P$ is the normal vector to the curve $C_P$.

The term $\int_{C_P} (K_Q(f(s)) - K_P(s))^2 \, ds$ measures the difference between the curvature of the two curves. This induces a non convexity of the functional $E$. Consequently, solving the partial differential equation (6) will give us a local minimum of $E$. To overcome this problem we will assume that we have an initial estimation $f_0$ which is a good approximation of the real solution (the definition of the initial estimation $f_0$ will be explained later). This initial estimation defines a starting point for the search of a local minimum of the functional $E$. To take into account this initial estimation we consider the associated evolution equation:

$$\begin{cases} \frac{\partial f(s)}{\partial t} + f''(s) \, \|Q'(f(s))\|^2 + K_P(s) \langle N_P(s), Q'(f(s)) \rangle + \frac{1}{R} [K_P(s) - K_Q(f(s))] \, K'_Q(f(s)) = 0 \\ f(0,s) = f_0(s) \text{ Initial estimation.} \end{cases} \tag{7}$$

Equation (7) can also be seen as a gradient descent algorithm toward a minimum of the energy $E$, it is solved by a finite element method and leads to the solution of a sparse linear system (see for more details [4]).

### 3.1 Determining the Initial Estimation $f_0$

The definition of the initial estimation $f_0$ has an effect upon the convergence of the algorithm. Consequently a good estimation of the solution $f$ will lead to a fast convergence. The definition of $f_0$ is based on the work of Duncan *et al* [8]. The method is as follows:

Let $s_i \in [0,1]$, $i = 1 \ldots n$ be a subdivision of the interval $[0,1]$. For every point $P_i = (X(s_i), Y(s_i))$ of the curve $C_P$ we search for a point $Q_i = (X(s'_i), Y(s'_i))$ on the curve $C_Q$, and the function $f_0$ is then defined by $f_0(s_i) = s'_i$.

For doing so we have to define a pair of points $P_0, Q_0$ which correspond to each other. But, first of all, let us describe the search method. In the following, we identify a point and its arc length (*i.e.* the point $s_i$ denotes the point $P_i$ of the curve $C_P$ such that $P(s_i) = P_i$, where $P$ is the parametrization of the curve $C_P$).

For each point $s_i$ of $C_P$ we associate a set of candidates $S_i$ on the curve $C_Q$. The set $S_i$ defines the search area. This set is defined by the point $s'$ which is the nearest distance point to $s_i$ belonging to the curve $C_Q$, along with $(N_{search} - 1)/2$ points of the curve $C_Q$ on each side of $s'$ (where $N_{search}$ is a given integer defining the length of the search area).

Among these candidates, we choose the point which minimizes the deformation energy (1).

In some situations this method fails, and the obtained estimation $f_0$ is meaningless, leading to a bad solution. Figure 1 shows an example where the method described in [8] fails. This is due to the bad computation of the search area $S_i$.

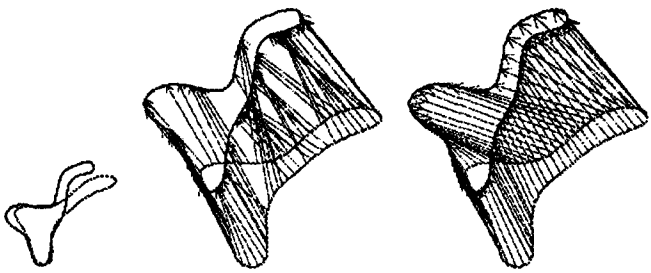

**Fig. 1.** This example shows the problem that can occur in the computation of the initial estimate based only on the search in a given area. The initial estimation of the displacement field and the obtained solution.

To compute more accurately this set, we have added a criterion based on the arc length. Consequently, the set defining the search area $S_i$ is defined by the point $s'$ which is the nearest distance point to $s_i$ belonging to the curve $C_Q$ such that $s'_i \approx s_i/\alpha$, along with $(N_{search} - 1)/2$ points of the curve $C_Q$ on each side of $s'_i$. Figure 2 illustrates the use of this new definition of the set $S_i$ for the same curves given in Fig. 1. This example shows the ability to handle more general situations with this new definition of the search area $S_i$.

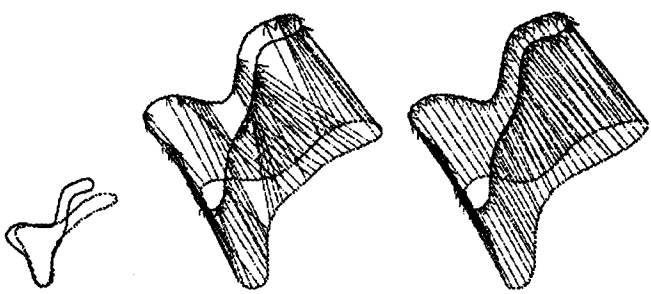

**Fig. 2.** In the same case of the previous example, the computation of the initial estimate based on the local search and the curvilinear abscissa, gives a good estimation $f_0$, which leads to an accurate computation of the displacement function.

As noted above, the search area $S_i$ can be defined only if we have already chosen a point $P_0$ and its corresponding point $Q_0$. The most salient features in a temporal sequence undergo small deformations at each time step, thus a good method for choosing the point $P_0$ is to take the most distinctive point so that the search for the corresponding point becomes a trivial task. Consequently the point $P_0$ is chosen among the points of $C_P$ with maximal curvature. In many cases this method provides a unique point $P_0$. Once we have chosen the point $P_0$, the point $Q_0$ is found by the local search described above.

## 4 Experimental Results

The method was tested on a set of synthetic and real image sequences. The results are given by specifying at each discretization point $P_i \quad i = 1 \ldots N$ of the curve $C_P$ the displacement vector $\mathbf{u_i} = \mathbf{P_i Q_i}$. At each point $P_i$ the arrow represents the displacement vector $\mathbf{u_i}$.

The first experiments were made on synthetic data. In Fig. 3, the curve $C_Q$ (a square) is obtained by a similarity transformation (translation, rotation and scaling) of the curve $C_P$ (a rectangle). The obtained displacement field and a plot of the function $f$ are given. We can note that the algorithm computes accurately the displacements of the

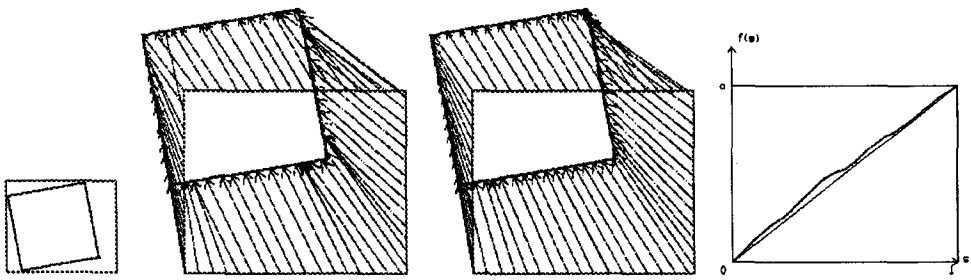

**Fig. 3.** The rectangle (in grey) is deformed by a similarity (translation, rotation and scaling) to obtain the black square. In this figure we represent the initial estimation of the displacement vector of the curves, the obtained displacement field and the plotting of the solution $f$.

four corners. This result was expected since the curves $C_P$ and $C_Q$ have salient features which help the algorithm to compute accurately the displacement vector $\mathbf{u_i}$. Figure 4 give an example of the tracking of each point on an ellipse deformed by a similarity. In this case, the points of high curvature are matched together although the curvature varies smoothly.

As described in section (3.1) the computation of the initial estimation is crucial. In the following experimentation we have tried to define the maximal error that can be done on the estimation of $f_0$ without disturbing the final result. In Fig. 5 we have added a gaussian noise ($\sigma = 0.05$) to a solution $f$ obtained by solving (7). This noisy function was taken as an initial estimation for Eq. 7. After a few iterations the solution $f$ is recovered (5).

It appears that if $|f - f_0| \leq 4h$ (where $h$ is the space discretization step), starting with $f_0$ the iterative scheme 7 will converge toward the solution $f$. The inequality $|f - f_0| \leq 4h$ means that for each point $P$ on the curve $C_P$ the corresponding point $Q$ can be determined with an error of 4 points over the grid of the curve $Q$.

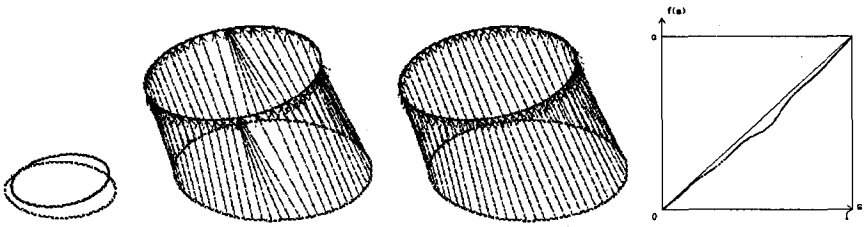

**Fig. 4.** Another synthetic example, in this case the curvature along the curves $C_P$ and $C_Q$ varies smoothly. This often produces as a consequence in the computation of the initial estimation $f_0$ that several points of the curve $C_P$ (in grey) match the same point of $C_Q$ (in black). We remark that, for the optimal solution obtained by the algorithm, each point of the black curve matches a single point of the grey curve, and that, maximum curvature points are matched together.

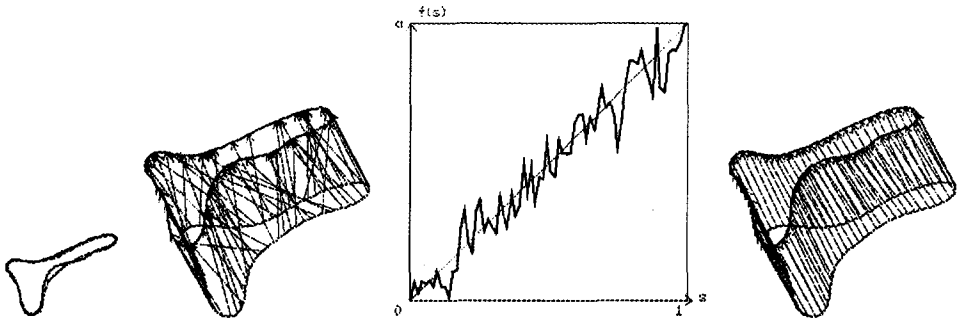

**Fig. 5.** In this example we have corrupted an obtained solution with a gaussian noise ($\sigma = 0.05$) and considered this corrupted solution as an initial estimate $f_0$. The initial displacement field, the initial estimate $f_0$ and the obtained solution are shown in this figure.

The tracking of the moving boundaries of the valve of the left ventricle on an ultrasound image helps to diagnose some heart diseases. The segmentation of the moving boundaries over the whole sequence was done by the snake model [6, 2, 10]. In Fig 6 a global tracking of a part of the image sequence is showed[2]. This set of curves are processed (as described in [4]) to obtain the curvatures and the normal vector of the curves. The Fig. 7 shows a temporal tracking of some points of the valve in this image sequence. The results are presented by pairs of successive contours. One can visualize that the results meet perfectly the objectives of preserving the matching of high curvature points while insuring a smooth displacement field.

[2] Courtesy of I. Herlin [10]

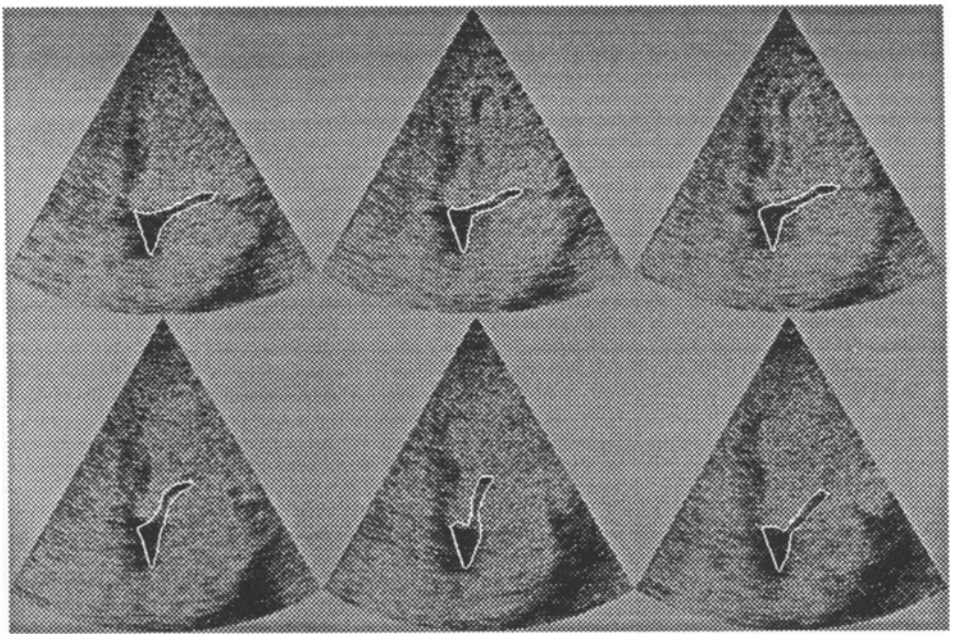

**Fig. 6.** Temporal tracking of the mitral valve, obtained by the snake model [10], for images 1 to 6.

## 5 3-D Generalization

In this section we give a 3-D generalization of the algorithm described in the previous sections. In 3-D imaging we must track points on located surfaces, since the objects boundaries are surfaces (as in [1]). In [16] the authors have shown on a set of experimental data, that the extrema of the larger principal curvature often correspond to significant intrinsic (i.e. invariant by the group of rigid transformation) features which might characterize the surface structure, even in the presence of small anatomic deformations.

Let $S_P$ and $S_Q$ be two surfaces parameterized by $P(s,r)$ and $Q(s',r')$, and let $\kappa_P$ denote the larger value of the principal curvature of the surface $S_P$ at point $P$.

Thus the matching of two surfaces, leads to the following problem:

find a function

$$f : \mathbb{R}^2 \rightarrow \mathbb{R}^2; \quad (s,r) \mapsto (s',r')$$

which minimizes the functional:

$$E(f) = \int_{S_P} (\kappa_Q(f(s,r)) - \kappa_P(s,r))^2 ds dr + R_s \int_{S_P} \left\| \frac{\partial (Q(f(s,r)) - P(s,r))}{\partial s} \right\|^2 ds dr + R_r \int_{S_P} \left\| \frac{\partial (Q(f(s,r)) - P(s,r))}{\partial r} \right\|^2 ds dr$$

where $\|.\|$ denotes the euclidean norm in $\mathbb{R}^3$. Its resolution by a finite element method can be done as in [5], and the results should be compared to those obtained by [1]. This generalization has not been implemented yet.

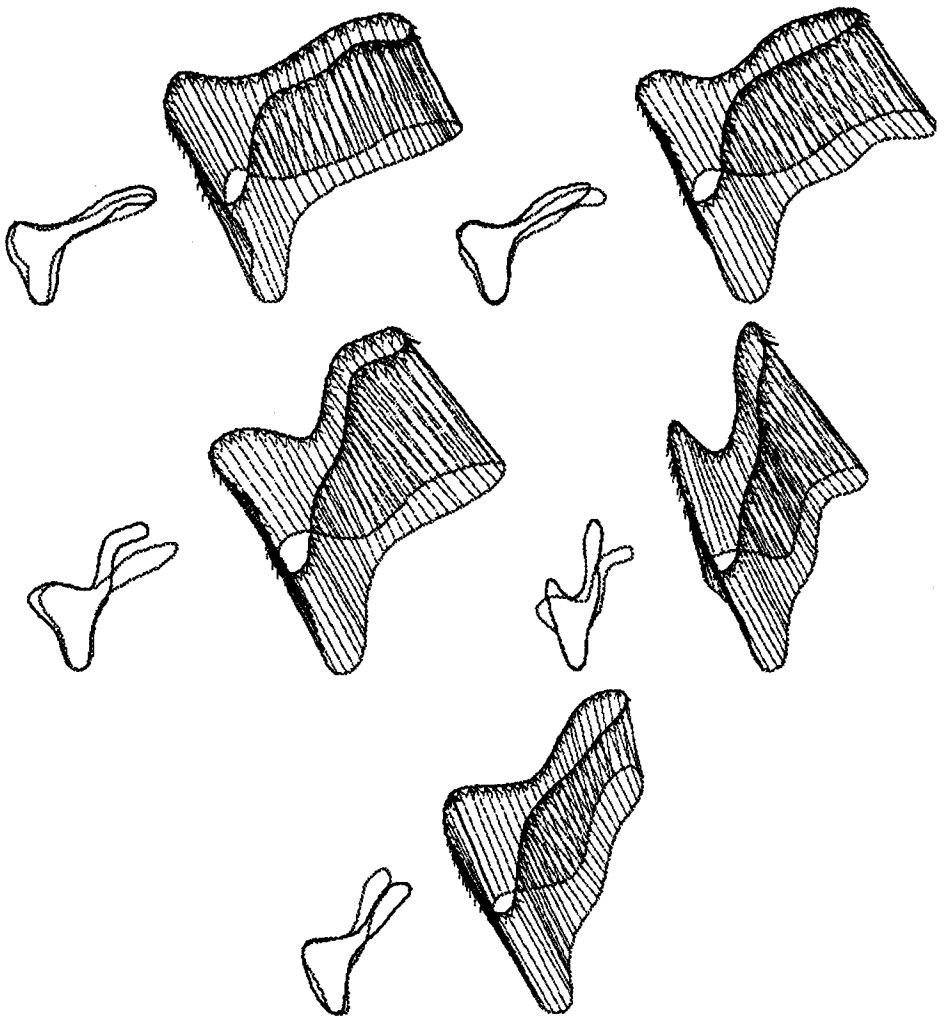

**Fig. 7.** Applying the point - tracking algorithm to the successive pairs of contours of Fig. 6 (from left to right and top to bottom).

## 6 Conclusion

We presented a significant improvement to Duncan's team approach to track the motion of deformable 2D shapes, based on the tracking of high curvature points while preserving the smoothness of the displacement field. This approach is an alternative to the other approaches of the literature, when no physical or geometric model is available, and can also be used as a complementary approach otherwise.

The results on a real sequence of time varying anatomical structure of the beating heart perfectly met the defined objectives [2]. Future work will include the experimentation of the 3-D generalization.

## References


1. A. Amini, R. Owen, L. Staib, P. Anandan, and J. Duncan. *non-rigid motion models for tracking the left ventricular wall.* Lecture notes in computer science: Information processing in medical images. 1991. Springer-Verlag.
2. Nicholas Ayache, Isaac Cohen, and Isabelle Herlin. Medical image tracking. In *Active Vision,* Andrew Blake and Alan Yuille, chapter 20. MIT Press, 1992. In press.
3. Fred L. Bookstein. Principal warps: Thin-plate splines and the decomposition of deformations. *IEEE Transactions on Pattern Analysis and Machine Intelligence*, PAMI-11(6):567–585, June 1989.
4. Isaac Cohen, Nicholas Ayache, and Patrick Sulger. Tracking points on deformable objects using curvature information. Technical Report 1595, INRIA, March 1992.
5. Isaac Cohen, Laurent D. Cohen, and Nicholas Ayache. Using deformable surfaces to segment 3-D images and infer differential structures. *Computer Vision, Graphics, and Image Processing: Image Understanding*, 1992. In press.
6. Laurent D. Cohen and Isaac Cohen. A finite element method applied to new active contour models and 3-D reconstruction from cross sections. In *Proc. Third International Conference on Computer Vision*, pages 587–591. IEEE Computer Society Conference, December 1990. Osaka, Japan.
7. Court B. Cutting. Applications of computer graphics to the evaluation and treatment of major craniofacial malformation. In Jayaram K.Udupa and Gabor T. Herman, editors, *3-D Imaging in Medicine.* CRC Press, 1989.
8. J.S. Duncan, R.L. Owen, L.H. Staib, and P. Anandan. Measurement of non-rigid motion using contour shape descriptors. In *Proc. Computer Vision and Pattern Recognition*, pages 318–324. IEEE Computer Society Conference, June 1991. Lahaina, Maui, Hawaii.
9. A. Guéziec and N. Ayache. Smoothing and matching of 3D-space curves. In *Proceedings of the Second European Conference on Computer Vision 1992*, Santa Margherita Ligure, Italy, May 1992.
10. I.L. Herlin and N. Ayache. Features extraction and analysis methods for sequences of ultrasound images. In *Proceedings of the Second European Conference on Computer Vision 1992*, Santa Margherita Ligure, Italy, May 1992.
11. Ellen Catherine Hildreth. *The Measurement of Visual Motion.* The MIT Press, Cambridge, Massachusetts, 1984.
12. Bradley Horowitz and Alex Pentland. Recovery of non-rigid motion and structures. In *Proc. Computer Vision and Pattern Recognition*, pages 325–330. IEEE Computer Society Conference, June 1991. Lahaina, Maui, Hawaii.
13. L.D. Landau and E.M. Lifshitz. *Theory of elasticity.* Pergamon Press, Oxford, 1986.
14. Dimitri Metaxas and Demetri Terzopoulos. Constrained deformable superquadrics and nonrigid motion tracking. In *Proc. Computer Vision and Pattern Recognition*, pages 337–343. IEEE Computer Society Conference, June 1991. Lahaina, Maui, Hawaii.
15. Sanjoy K. Mishra, Dmitry B. Goldgof, and Thomas S. Huang. Motion analysis and epicardial deformation estimation from angiography data. In *Proc. Computer Vision and Pattern Recognition*, pages 331–336. IEEE Computer Society Conference, June 1991. Lahaina, Maui, Hawaii.
16. O. Monga, N. Ayache, and P. Sander. From voxel to curvature. In *Proc. Computer Vision and Pattern Recognition*, pages 644–649. IEEE Computer Society Conference, June 1991. Lahaina, Maui, Hawaii.